Verification of Ising phase transitions in the three-dimensional Ashkin-Teller model using Monte Carlo simulations

G. Szukowski, G. Kamieniarz, and G. Musiał*
Faculty of Physics, A. Mickiewicz University, ulica Umultowska 85, 61-614 Poznań, Poland
(Received 3 January 2008; published 21 March 2008)

Monte Carlo simulations in the three-dimensional (3D) Ashkin-Teller model on a cubic lattice are performed in the regions of the two-parameter space diagram where Ising-type phase transitions are expected. The scaling behavior of the Binder cumulant Q and the magnetic susceptibility in the critical region are exploited. In simulations the periodic boundary conditions and the Metropolis algorithm are used. Starting from Ising critical exponents and applying the finite-size-scaling analysis of the cumulant Q with nonlinear corrections, the accurate positions of the critical couplings on the continuous phase transition lines are calculated. For these couplings the critical exponent y_h is calculated analyzing the magnetic susceptibility in the framework of the finite-size scaling with corrections. The values of y_h agree with the 3D Ising model value along two lines determined by the order parameter $\langle s\sigma\rangle$.

DOI: 10.1103/PhysRevE.77.031124 PACS number(s): 05.50.+q, 75.10.Hk, 75.30.Kz, 75.40.Mg

I. INTRODUCTION

As a nontrivial generalization of the Ising model, the Ashkin-Teller (AT) model [1] has been for many decades one of the important reference points in statistical physics. The interest in this model has much increased after Fan's paper appeared [2] in which he expressed the Hamiltonian H of this model

$$-\frac{H}{k_BT}=\sum_{[i,j]}\{K_2(s_is_j+\sigma_i\sigma_j)+K_4s_i\sigma_is_j\sigma_j\} \tag{1}$$

by means of two independent Ising degrees of freedom, s_i and σ_i (i.e., s_i and σ_i are the variables that can take values +1 or −1), residing on each lattice site. $[i,j]$ denotes the summation over nearest neighboring lattice sites, $K_i=-J_i/k_BT$, with $i=2$ or 4, and T is temperature. Moreover, J_2 is the coupling of the nearest neighbor interaction between the degrees of freedom s_i as well as for σ_i, whereas J_4 is the coupling between the product of these degrees of freedom $s_i\sigma_i$.

This model can be interpreted as two superimposed Ising models and this fact prompted the interest in its critical properties (see [3–9], and the papers cited therein). One of the models is described in spin variables s_i and the other in variables σ_i and in both of them there are exclusively two-spin interactions of a constant magnitude J_2 between the nearest neighbors only. Simultaneously, these two different models are coupled by a four-spin interaction of a constant magnitude J_4, also only between couples of spins residing at the nearest neighboring lattice sites. Thus, this is a model with a three-component order parameter: $\langle s\rangle$, $\langle\sigma\rangle$, and $\langle s\sigma\rangle$, where the symbol $\langle\cdots\rangle$ denotes the thermal average. Moreover, the symbol $\langle s\sigma\rangle$ means that we calculate the thermal average of the variable $s\sigma$ being the product of the spins s and σ, residing on the same lattice site. These three parameters can be ordered independently leading to the interesting phase diagram.

The present state of knowledge about the phase diagram of the three-dimensional (3D) Ashkin-Teller model on a cubic lattice is presented in Fig. 1. The broken and solid lines denote the first order and the continuous phase transitions, respectively. The first thorough analysis by both the short series analysis and the Monte Carlo (MC) method and discussion of the phase diagram was made by Ditzian *et al.* [3]. In Fig. 1 all phases are specified in the legend and we follow the notation of Ditzian *et al.* [3]. In [3] the reader finds also an interesting comparative discussion which brackets the behavior of the 3D AT model between the mean field and the two-dimensional (2D) behaviors. We see from the above that the phase diagrams of the AT model in 2D and in 3D substantially differ. The precise MC results of Arnold and Zhang

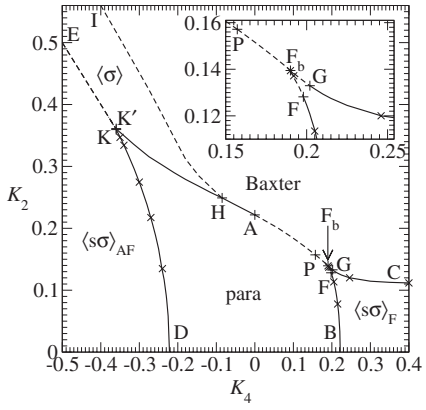

FIG. 1. The phase diagram of the 3D Ashkin-Teller model on a cubic lattice. The broken lines denote the first order phase transitions, whereas the solid lines denote the continuous ones. The phase labeled Baxter is ferromagnetically ordered with $\langle s\rangle$, $\langle\sigma\rangle$, and $\langle s\sigma\rangle$ nonzero, whereas in the phase labeled para they are all zero. In the phases "$\langle s\sigma\rangle_F$" and "$\langle s\sigma\rangle_{AF}$," $\langle s\rangle=\langle\sigma\rangle=0$, and only the parameter $\langle s\sigma\rangle$ is ferromagnetically and antiferromagnetically ordered, respectively. For the phase "$\langle s\rangle$," $\langle s\sigma\rangle=0$ and either $\langle s\rangle$ or $\langle\sigma\rangle$ is ferromagnetically ordered but the other is not. The positions of labeled points inside the phase diagram are marked by +'s, whereas the results of our Monte Carlo simulations are marked with ×'s.

*Corresponding author; gmusial@amu.edu.pl

[4] were obtained in the narrow range of the model parameters along the line AP (with P being the four state Potts point). The boundaries of the mixed phase region $\langle s \rangle$ and the localization of the tricritical point H were investigated and the deviations from the Ising character of phase transitions on the line AHK' were reported by Musiał and Rogiers [10], whereas the localization of the remaining tricritical points K, K',F,G were examined by Musiał [11].

Apart from the interesting and complicated phase diagram (the tricritical points, weakly first order phase transitions in the surrounding of point A, the mixed phase region "$\langle s \rangle$," and a possible variation of values of critical exponents along the line AHK') and the fact that this model is being used for interpretation of the experimental data [5], it still is an important reference point in the statistical physics and it has found many interesting applications from cosmology [4] to neural networks [12].

Recently the critical properties of the 3D Ising models were carefully investigated by Deng and Blöte [13] using the cluster MC method. Their precise results for the Ising universality class can be exploited here as far as the critical exponents and the critical value of the Binder cumulant are concerned. Recent extensions of the MC simulations to other important spin lattice models (tricritical Blume-Capel and dilute Potts models) [14–16] are worth noting.

This paper presents the results of our MC simulations in these regions of the (K_4, K_2) phase diagram of the 3D AT model on a cubic lattice in which the bibliographical data suggest the Ising character of phase transitions. The new motivation to continue the work done in the papers [11,17] toward confirmation of the Ising universality class of the continuous phase transition lines of the model (1) comes from the achievements of Deng and Blöte [13]. Their data and our accurate calculations of the phase transition points together with the careful finite-size-scaling analysis of the magnetic susceptibility have prompted us to estimate the value of the critical exponent y_h in agreement with the corresponding Ising value.

As in our previous simulations, we have used the local Metropolis algorithm suffering from critical slowing down, although more efficient cluster algorithms have been worked out [18,19] for the Ashkin-Teller model. In two dimensions they suppress [20] critical slowing down. In three dimensions, where for Ising-type models it is only partially reduced [19], cluster algorithms would nevertheless improve the efficiency of simulations.

II. MONTE CARLO SIMULATIONS

The Monte Carlo simulation is a kind of experiment performed to predict the behavior of a macroscopic system (i.e., that with a large number of degrees of freedom) when given the laws governing its microscopic behavior. Here each MC run started with thermalization of the length of 10^7 Monte Carlo steps (MCS) to reach thermodynamic equilibrium assuming the periodic boundary conditions. Our MCS is completed when each of the lattice sites has been visited once.

Next, we have generated the equilibrium configurations (microstates) of the finite-size cubic spin samples of the size $L \times L \times L$ $(8 \leq L \leq 30)$ for fixed values of the model parameters, using the Metropolis algorithm. The good quality 64-bit random number generator was exploited, applicable even in parallel processing, as checked by Srinivasan *et al.* [21]. It was important to have independent sets of pseudorandom numbers in each parallel process to obtain statistically independent results.

Each MC run was split into $k=19$ segments, each of them consisting of five 5×10^6 MCS and one partial average of each measured quantity (PA) was calculated from microstates in each segment to estimate the statistical scattering of the results. In the calculation of PAs only every tenth MC step contributes, to avoid correlations between sampled microstates of spins in the system and to sample microstates with the Gibbs distribution of probability.

To determine the phase transition points, an analysis of behavior of the fourth order cumulant Q_L is convenient [6,13,22].

$$Q_L = \frac{\langle M_\alpha^2 \rangle_L^2}{\langle M_\alpha^4 \rangle_L}, \tag{2}$$

where $\langle M_\alpha^n \rangle_L$ denotes the nth power of the α spins order parameter, with $\alpha = s$, σ, or $s\sigma$, averaged over an assembly of independent samples of the size $L \times L \times L$. The cumulant Q_L, called the Binder cumulant, allows investigation of the magnetic ordering in a system, as for $T > T_c$ and $L \gg \xi$, where ξ denotes the correlation length, Q_L tends toward $\frac{1}{3}$, which corresponds to a Gaussian distribution, whereas for $T < T_c$ and $L \gg \xi$, Q_L tends to 1 [22,23]. In the critical region for $L \approx \xi$, Q_L varies only weakly with temperature and linear dimension, and stays very close to the constant value Q. For the 3D Ising model with cubic symmetry and periodic boundary conditions, Deng and Blöte [13] have obtained $Q = 0.623\,41(4)$, achieved at the critical point in the thermodynamic limit $L \to \infty$.

The critical value of the cumulant Q_L is useful for determination of critical points also in the AT model, reducing the number of unknown parameters in the fitting procedure. Neglecting corrections to scaling, the critical value K_{2c} can be estimated from the common intersection point of the curves Q_L [6,22,23], having fixed the value K_{4c}.

An improvement of this estimation can be achieved if the nonlinear corrections to scaling [24] are taken into account. Fixing the value of the coupling K_4, we can write the corresponding expansion in the form [24]

$$Q_L(K_2) = Q + a_1(K_2 - K_{2c})L^{y_t} + a_2(K_2 - K_{2c})^2 L^{2y_t} + \cdots + b_1 L^{y_i} + b_2 L^{y_2} + \cdots, \tag{3}$$

applicable when $x \equiv (K_2 - K_{2c})L^{y_t} \ll 1$, where a_i and b_i are nonuniversal coefficients, $y_2 = d - 2y_h$, and $d=3$ is the dimensionality of the system. The recently obtained values of critical exponents for the 3D Ising universality class [13] are $y_t = 1.5868(3)$, $y_h = 2.4816(1)$, $y_i = -0.821(5)$, and the universal ratio $Q = 0.623\,41(4)$.

In the critical regions, a similar scaling analysis of the magnetic susceptibility of α spins calculated for the finite-size samples

$$\chi_L = L^d \langle M_\alpha^2 \rangle_L^2 \tag{4}$$

can be performed. Fixing the value of the coupling K_4, the expansion in $x \equiv (K_2 - K_{2c}) L^{y_t} \ll 1$,

$$\chi_L(K_2) = c_0 + L^{2y_h - d}[e_0 + e_1(K_2 - K_{2c})L^{y_t} + e_2(K_2 - K_{2c})^2 L^{2y_t} + b_1 L^{y_i}] \tag{5}$$

can be found [24], where b_i, c_i, e_i are nonuniversal coefficients and the remaining parameters have the same meaning as in Eq. (3). The analysis based on the expansion (5) leads to good estimates of the critical exponent y_h provided that K_{2c} is known to a high accuracy.

III. SIMULATION RESULTS AND THEIR ANALYSIS

We have performed simulations in the regions of the phase diagram close to the lines DK, BF, and CG in Fig. 1 where the Ising character can be anticipated (see [10,11], and the papers cited therein). Musiał and Rogiers have found [10] that the phase transitions on the line AHK' are probably also continuous but they do not seem to be Ising type. To analyze the phase transitions on the lines DK, BF, and CG in Fig. 1 we use the mean values of spins s, σ, and $s\sigma$ as the order parameters.

In the first step, for a given value of K_4 coupling, we have obtained the initial localization of the coupling K_{2c} using the common intersection point of the curves Q_L corresponding to the linear approximation to scaling expansion (3). In this way, we have confirmed the value of K_{2c} previously obtained [11,17] with the precision of an order 10^{-4}. This accuracy was not enough for us as the real scaling variable was $x = (K_2 - K_{2c}) L^{y_t}$ and increased with L.

In the second step we take into account the nonlinear corrections in scaling expansion (3) assuming the Ising critical exponents [13]. The formula (3) is transformed to the form

$$Q_L - b_1 L^{y_i} - b_2 L^{y_2} = Q + a_1 x + a_2 x^2, \tag{6}$$

very convenient for analysis thanks to the fact that all data obtained for $Q_L(K_2)$ as a function of $x = (K_2 - K_{2c}) L^{y_t}$ (at fixed K_4) should collapse now on the same parabola. This makes the fitting procedure very effective and transparent.

Examples of such analyses are shown in Figs. 2–5. Figures 2 and 3 demonstrate the use of the finite-size scaling formula in the form (6) at the coupling $K_4 = 0.205$ when we leave Q as the free parameter being the subject of fitting. In Fig. 2 no correction terms with nonuniversal amplitudes b_i are taken and one can see that the MC data are not convergent to the curve (6) within the fitting error bars and depend on the size L. Moreover, the fitted value $Q = 0.647(2)$ does not agree with the expected value $Q = 0.623\,41(4)$ [13].

In the presence of the correction terms with nonuniversal amplitudes b_i, the same MC data presented now in Fig. 3 are convergent to the estimate $Q = 0.625(2)$, which agrees with the expected value $Q = 0.623\,41(4)$ [13] within the fitting error bars, and lead to $K_{2c} = 0.1135(3)$.

Next we take the Ising value for the parameter Q obtaining the improved results for critical value of the coupling K_2. The corresponding finite-size scaling analysis is shown in Fig. 4 for $K_{4c} = 0.205$. The same numerical data as those in Figs. 2 and 3 are reassembled due to a small modification of the critical coupling $K_{2c} = 0.113\,71(5)$ for comparison. They

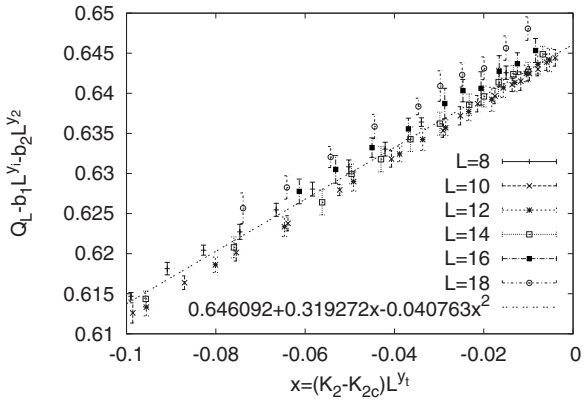

FIG. 2. Illustration of the finite-size scaling analysis of $Q_L(K_2)$ at the fixed value $K_{4c} = 0.205$ when Q is the free parameter and no correction terms with nonuniversal amplitudes b_i are taken, i.e., $b_1 = b_2 = 0$ here. The system size L and the fitted parabola, marked by the broken line, are displayed in the legend box.

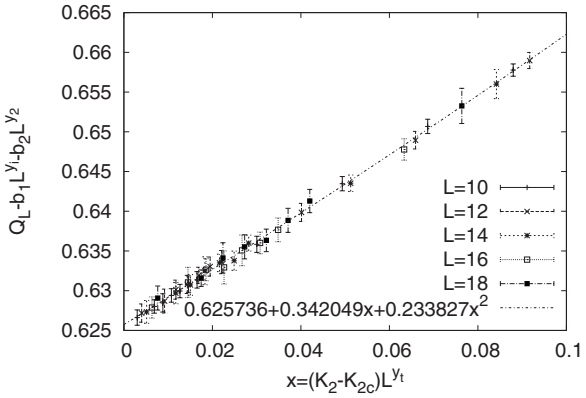

FIG. 3. Illustration of the finite-size scaling analysis of $Q_L(K_2)$ at $K_{4c} = 0.205$ when Q is subject to fitting. The system size L and the fitted parabola, marked by the broken line, are displayed in the legend box.

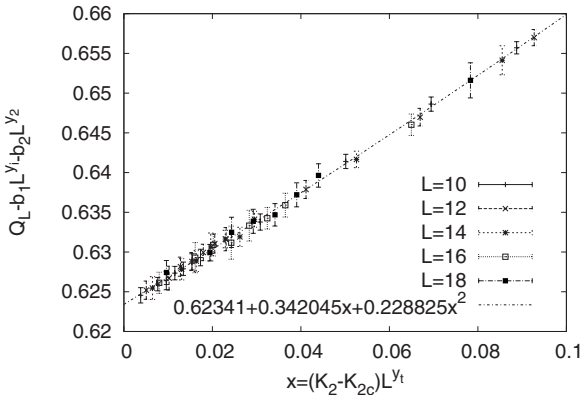

FIG. 4. The finite-size scaling analysis of $Q_L(K_2)$ at $K_{4c} = 0.205$ when Q is set to the universal value $Q = 0.623\,41$. The system size L and the fitted parabola, marked by the broken line, are displayed in the legend box.

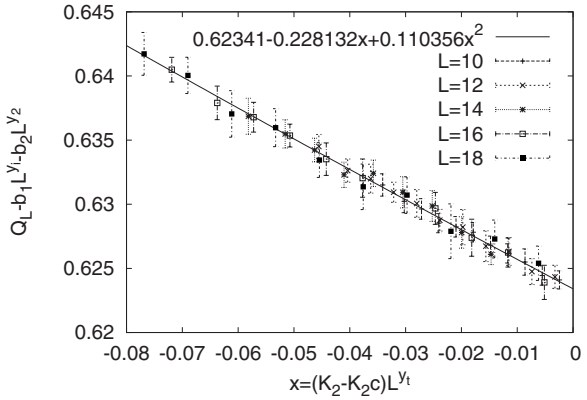

FIG. 5. The finite-size scaling analysis of $Q_L(K_2)$ at the antiferromagnetic coupling $K_{4c}=-0.24$ when Q is set to the universal value $Q=0.623\,41$. The obtained value $K_{2c}=0.134\,887(8)$. The system size L and the fitted parabola, marked by the broken line, are displayed in the legend box.

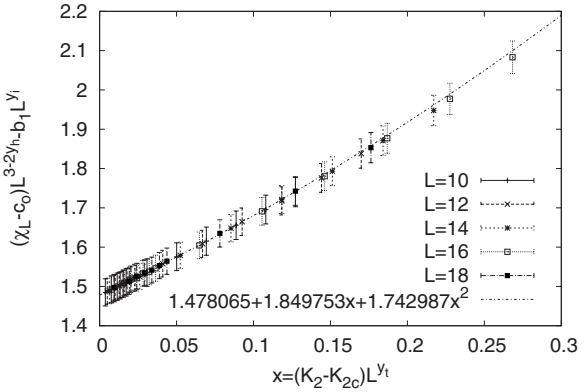

FIG. 6. Demonstration of the use of Eq. (7) for the finite-size scaling analysis of the $\chi_L(K_2)$ dependence at the fixed values $K_{4c}=0.205$ and $K_{2c}=0.113\,48$. The estimated value of the critical exponent y_h is 2.49(1). The system size L and the fitted parabola, marked by the broken line, are displayed in the legend box.

fulfill the scaling law very well for $0.003 \leq x \leq 0.3$. The fitting procedure and scaling properties in the antiferromagnetic region of the phase diagram are shown in Fig. 5.

The results of our analyses performed within the finite-size scaling formula (3) down to $|x|=0.002$ are collected in Table I. The first two columns display the coordinates K_{4c} and K_{2c} of the critical points and they are also marked by $\times$'s in the phase diagram plotted in Fig. 1. The next columns in Table I list the values of nonuniversal coefficients a_1, a_2, b_1, and b_2 with the uncertainties given in parentheses. The precision of calculation of K_{2c} is five or even six digits except the points close to the tricritical points K and F, at which it is of four digits, supposedly as a result of the crossover behavior.

High precision of the critical values K_{2c} for a given K_{4c} has enabled the accurate finite-size scaling analysis of magnetic susceptibility. The expression (5) here is also transformed to the form

$$[\chi_L - c_0]L^{d-2y_h} - b_1 L^{y_i} = e_0 + e_1 x + e_2 x^2, \tag{7}$$

which separates the part dependent on the scaling variable x from that depending on L. Thus, all data obtained for $\chi_L(K_2)$ at fixed K_4 and arbitrary L should fit the same parabola.

An example of such an analysis with the finite-size scaling formula (7) and $K_4=0.205$ (the same value as in Figs. 2–4 for consistency) is illustrated in Fig. 6. The scaling law is fulfilled in the region $0.005 \leq x \leq 0.27$. This analysis leads to estimates of the critical exponent y_h with the precision of three significant digits.

The final results are collected in Table II. The first column gives the coordinates of K_{4c} to which the results refer. The second column displays the estimated values of the critical exponent y_h, and the next columns present the values of nonuniversal coefficients c_0, e_0, e_1, e_2, and b_1 in the expansions (5) and (7). For convenience, the data referring to the lines KD, FB, and GC of the phase diagram shown in Fig. 1 are separated by horizontal lines, respectively. For the phase

TABLE I. The critical couplings K_{4c} and K_{2c} together with the values of nonuniversal coefficients a_1, a_2, b_1, and b_2 in the finite-size scaling expansion (3) for the 3D Ashkin-Teller model. The data referring to the lines KD, FB, and GC in the phase diagram shown in Fig. 1 are separated by horizontal lines, respectively.

K_{4c}	K_{2c}	a_1	a_2	b_1	b_2
−0.35	0.3470(1)	−1.18(3)	−0.55(2)	−0.54(3)	−0.26(9)
−0.34	0.334158(6)	−0.97(1)	1.6(1)	−0.02(2)	−3.4(2)
−0.3	0.274644(4)	−0.57(1)	−0.06(3)	0.08(1)	−0.5(1)
−0.27	0.21739(1)	−0.40(1)	0.15(2)	0.07(1)	−0.06(1)
−0.24	0.134887(8)	−0.23(1)	0.04(2)	0.090(3)	−0.05(3)
0.19	0.1394(2)	2.0(9)	6(3)	1.0(3)	−3.2(2)
0.192	0.1371(1)	1.5(3)	2.6(4)	0.33(4)	1.1(6)
0.205	0.11371(5)	0.35(1)	0.16(7)	0.078(2)	0.29(2)
0.215	0.07769(3)	0.163(2)	0.056(4)	0.098(2)	0.10(4)
0.246	0.120040(7)	1.72(5)	3.2(3)	0.07(2)	−0.3(2)
0.4	0.111760(7)	1.74(1)	3.3(1)	0.11(2)	−0.23(3)

TABLE II. The critical exponent y_h for particular values of the coupling K_{4c} together with the values of nonuniversal amplitudes c_0, e_0, e_1, e_2, and b_1 in the expansion (5). The data referring to the lines *KD*, *FB*, and *GC* in the phase diagram shown in Fig. 1 are separated by horizontal lines, respectively.

K_{4c}	y_h	c_0	e_0	e_1	e_2	b_1
−0.35	2.52(2)	14.3(4)	9.83(1)	−4.31(3)	4.32(9)	1.03(7)
−0.34	2.47(2)	14.4(4)	1.66(4)	−5.03(7)	6.42(8)	0.1(1)
−0.3	2.52(4)	−8.6(9)	0.9(1)	−2.3(1)	1.1(1)	2.0(2)
−0.27	2.50(2)	−3.8(1)	1.14(2)	−1.82(1)	0.9(2)	1.0(1)
−0.24	2.51(3)	−7(2)	1.0(2)	−1.00(6)	0.2(2)	1.7(4)
0.19	2.7(2)	25(9)	2.2(7)	16(2)	39(5)	5.2(7)
0.192	3.0(2)	17(6)	1.8(2)	10(1)	23(7)	−1.6(5)
0.205	2.49(1)	1.0(4)	1.42(1)	1.84(1)	1.32(3)	1.2(3)
0.215	2.51(3)	−5.9(5)	0.9(1)	0.65(3)	0.6(3)	1.7(2)
0.246	2.8(2)	34(5)	1.37(8)	0.30(2)	0.51(5)	−2.6(4)
0.4	2.9(1)	−0.4(3)	0.963(3)	0.010(5)	0.02(1)	0.0067(4)

transition lines *KD* and *FB*, determined by the order parameter $\langle s\sigma\rangle$, the critical exponent agrees with the Ising value within error bar. The deviations occur only in close vicinity of the tricritical points *K* for $K_4=-0.35$ and *F* for $K_4=0.19$ and 0.192, which is not taken into account in the scaling expressions (3) and (5). The strong overestimation of y_h for the horizontal line *GC*, determined by the order parameters $\langle s\rangle$ and $\langle\sigma\rangle$, occurs and may be related to substantial deviations from the scaling behavior (5) and (7). We do not know if this is a signature of a different universality class, an artifact of our simulation algorithm, or the lack of higher order terms in Eq. (5).

IV. CONCLUSIONS

For the first time the corrections to scaling have been taken into account in the analysis of the MC simulation data for the Ashkin-Teller model. The sample sizes *L* were moderate but simulations were long enough to extract precise values of the cumulant ratio and magnetic susceptibility needed for the nonlinear data analysis. The quality of the simulation data has led to conservation of scaling laws by the scaling variable *x* over two to three decades of variation.

Using the finite-size scaling formula (3) and taking into account the Ising critical exponents and the critical point ratio *Q*, we have calculated the coordinates K_{4c} and K_{2c} in the phase diagram shown in Fig. 1 to a precision of five to significant six digits except for the points close to the tricritical points *K* and *F*, where this precision is four digits.

Having reached a sufficient level of accuracy for the critical coupling K_{2c}, we have calculated the critical exponent y_h to a precision of 1–4 %. For the phase transition lines *KD* and *FB*, determined by the order parameter $\langle s\sigma\rangle$, the estimated y_h values agree with that for the Ising universality class so that for the first time we have confirmed the 3D Ising behavior in this part of the Ashkin-Teller phase diagram. Despite the numerical effort, we have estimated y_h at about 2.8–2.9 for the critical points along the phase transition line *GC*, determined from the $\langle s\rangle$ and $\langle\sigma\rangle$ order parameter. We consider this result as an artifact rather than a signature of different critical behavior.

ACKNOWLEDGMENTS

The authors wish to thank the Poznań Supercomputing and Networking Center for access to the supercomputers, on which a significant part of the simulations has been performed. Partial financial support from the Polish Ministry of Science and Higher Education with Grants No. 8 T11F 027 16 and No. 1 P03B 037 30 is also acknowledged.

[1] J. Ashkin and E. Teller, Phys. Rev. **64**, 178 (1943).
[2] C. Fan, Phys. Lett. **39A**, 136 (1972).
[3] R. V. Ditzian, J. R. Banavar, G. S. Grest, and L. P. Kadanoff, Phys. Rev. B **22**, 2542 (1980).
[4] P. Arnold and Y. Zhang, Nucl. Phys. B **501**, 803 (1997).
[5] L. F. Feiner and A. M. Oleś, Phys. Rev. B **59**, 3295 (1999).
[6] P. Pawlicki, G. Kamieniarz, and L. Dębski, Physica A **242**, 290 (1997).
[7] R. J. Baxter, *Exactly Solvable Models in Statistical Mechanics* (Academic Press, London, 1982).
[8] G. Kamieniarz, P. Kozłowski, and R. Dekeyser, Phys. Rev. E **55**, 3724 (1997).
[9] P. Pawlicki, G. Musiał, G. Kamieniarz, and J. Rogiers, Physica A **242**, 281 (1997).
[10] G. Musiał and J. Rogiers, Phys. Status Solidi B **243**, 335 (2006).
[11] G. Musiał, Phys. Rev. B **69**, 024407 (2004).
[12] D. Bollé and P. Kozłowski, J. Phys. A **32**, 8577 (1999).
[13] Y. Deng and H. W. J. Blöte, Phys. Rev. E **68**, 036125 (2003).
[14] Y. Deng and H. W. J. Blöte, Phys. Rev. E **70**, 046111 (2004).

[15] C. J. Silva, A. A. Caparica, and J. A. Plascak, Phys. Rev. E **73**, 036702 (2006).
[16] X. Qian, Y. Deng, and H. W. J. Blöte, Phys. Rev. E **72**, 056132 (2005).
[17] G. Musiał L. Dębski, and G. Kamieniarz, Phys. Rev. B **66**, 012407 (2002).
[18] S. Wiseman and E. Domany, Phys. Rev. E **48**, 4080 (1993).
[19] J. Salas and A. D. Sokal, J. Stat. Phys. **85**, 297 (1996); **87**, 1 (1997).
[20] Y. Deng, W. Guo, and H. W. J. Blote, e-print arXiv:cond-mat/0605165; Y. Deng, T. M. Garoni, W. Guo, H. W. J. Blöte, and A. D. Sokal, Phys. Rev. Lett. **98**, 120601 (2007).
[21] A. Srinivasan, M. Mascagni, and D. Ceperley, Parallel Comput. **29**, 69 (2003).
[22] K. Binder and D. P. Landau, Phys. Rev. B **30**, 1477 (1984).
[23] K. Binder and D. W. Heerman, *Monte Carlo Simulation in Statistical Physics*, Springer Series in Solid State Physics Vol. 80 (Springer-Verlag, Berlin, 1988).
[24] H. W. J. Blöte, E. Luijten, and J. R. Heringa, J. Phys. A **28**, 6289 (1995); A. L. Talapov and H. W. J. Blöte, *ibid.* **29**, 5727 (1996).